

Original Paper

An Adaptive Robust Control Method for Chaotic State of Permanent Magnet Synchronous Motor

Wei Zhang¹ & Lingyan Chang^{1*}

¹ Department of Automotive Engineering, Yantai Engineering & Technology College, Yantai, Shandong 264000, China

* Corresponding author, Lingyan Chang, Department of Automotive Engineering, Yantai Engineering & Technology College, Yantai, Shandong 264000, China

Received: March 20, 2024

Accepted: April 21, 2024

Online Published: April 28, 2024

doi:10.22158/asir.v8n2p33

URL: <http://doi.org/10.22158/asir.v8n2p33>

Abstract

In this paper, a chaotic control method based on adaptive robust controller is proposed to solve the chaos phenomenon of the permanent magnet synchronous motor system by mathematically analyzing the dynamic model of the permanent magnet synchronous motor system to eliminate or suppress chaos in the permanent magnet synchronous motors. This method also takes into account the parameter uncertainties (structural uncertainties) of the system and the external load torque interference (unstructured uncertainty). The former is compensated by adaptive control, and the latter by robust term. Feedforward elimination technology can integrate them together, and effectively reduce the influence of chaos on system performance and realize the high precision position tracking of the permanent magnet synchronous motor system. The Lyapunov method is used to prove the stability of the controller. The simulation results show that the method is better in robustness and control precision.

Keywords

permanent magnet synchronous motor, chaos, adaptive robust control, parameter uncertainty, external disturbance

1. Introduction

With the development of permanent magnet materials, permanent magnet synchronous motor (PMSM) has been widely applied in the elevator, the ship electric propulsion and hybrid car and many other areas (Mark & Vairamani, 2014; Xu & Yao, 2001; Yao, Hu, & Wang, 2012). In recent years, however, the research results show that the permanent magnet synchronous motor within a fixed parameter range may appear chaotic behavior, which lead to low frequency oscillation, and irregular electromagnetic

noise problems, reducing stability of the system variation (Hemail, 1994; Li, Park, Joo, Zhang, & Chen, 2002; Saberi Nik & Gorder, 2013; Saberi Nik, Gorder, & Gambi, 2015; Chua & Chen, 2003; Jing, Yu, & Chen, 2004; Wang & Chau, 2009; Krishnendu & Urmila, 2013). Therefore, it is very necessary and urgent to design an efficient controller to control and eliminate the chaos of the Magnet Synchronous Motor System based on the analysis and understanding of the chaotic dynamic characteristics of this system.

Control system for permanent magnet synchronous motor chaotic state, scholars carried out extensive research both at home and abroad. Among various kinds of chaos control method, earlier OGY method (Ott, Grebogi, & Yorke, 1990) is proposed, the method using chaos occurs attractor in the unstable periodic orbit has the sensitivity to small parameter perturbation and ergodicity of chaos movement characteristic, adding the small parameter perturbation control quantity to chaotic systems to make the system state control on a fixed point. However, this method for the stability of the time is too long. Literature (Zhang, Chau, & Wang, 2013) in this paper, a time delay feedback control (TDFC) of permanent magnet synchronous motor chaotic control method, the method avoids some limiting factors of the open loop and nonlinear closed-loop control, for any goal, the transfer domain of chaotic system of the control is global, avoiding the complicated calculation about determining the scope of the transfer domain. The control target of this method, however, must be in the balance of the system or unstable periodic orbit, and time delay in reality is difficult to determine. Literature (Ren & Ding, 2006; Babaei, Nazarzadeh, & Faiz, 2008) proposed a nonlinear feedback control method to control limit cycle stability and amplitude of the controlled system according to actual needs. This approach, however, is only under the condition of parameter uncertainty, when the parameters change greatly, it significantly reduce the control performance. Aiming at this problem, a kind of adaptive nonlinear feedback control method is proposed by Literature (Hu, Liu, Ma, & Ullah, 2015; Yao, Jiao, Ma, & Yan, 2014; Yao, Bu, Reedy, & Chiu, 2000; Yao, Jiao, & Ma, 2014; Sun, Gao, & Kaynak, 2013; Underwood & Husain, 2010; Yao, Jiao, & Ma, 2015), an adaptive law of the method is designed to estimate the unknown parameters of permanent magnet synchronous motor, and eliminated by feedforward technology on the structure of the unknown parameters bringing uncertainty to compensate. However, existing in the system for permanent magnet synchronous motor, unstructured uncertainties, such as load torque disturbance in the system, the adaptive controller regards it as the known variables without processing. But in fact the load torque is usually unknown and changes over time. The unstructured uncertainties affects the precision of the permanent magnet synchronous motor motion control system and performance, when the unstructured uncertainties become larger, adaptive control can even lead to instability of the control system.

System for permanent magnet synchronous motor, parameter uncertainties and external disturbance torque, this paper proposes an adaptive robust control method of permanent magnet synchronous motor chaotic inhibition and high precision speed tracking control, the method at the same time considering the parameter uncertainty (structure uncertainty) and the external load torque disturbance (unstructured uncertainty). This method is used in adaptive control to compensate the former, the robust

compensation term the latter, and they are eliminated by feedforward technology integration together. The simulation results verify the effectiveness of the proposed method.

2. The Chaos Dynamic Property Analysis of PMSM

Permanent magnet synchronous motor system transformation model (Hu, Liu, Ma, & Ullah, 2015) describes as follows:

$$\begin{cases} \dot{x} = \sigma(y - x) - \tilde{T}_L \\ \dot{y} = (\mu - z)x - y + \tilde{u}_q \\ \dot{z} = -z + xy + \tilde{u}_d \end{cases} \quad (1)$$

Among them:

$$x = \frac{R}{L_q} \tilde{x}, \quad y = \frac{P_n L_q \psi_{fd}}{R B_{equ}} \tilde{y}, \quad z = \frac{P_n L_q \psi_{fd}}{R B_{equ}} \tilde{z}$$

$$\tilde{x} = \omega, \quad \tilde{y} = i_q, \quad \tilde{z} = i_d$$

$$\sigma = \frac{B_{equ} L_q}{J_{equ} R}, \quad \mu = \frac{P_n \psi_{fd}^2}{R B_{equ}}$$

$$\tilde{u}_d = \frac{P_n L_q \psi_{fd}}{R^2 B_{equ}} u_d, \quad \tilde{u}_q = \frac{P_n L_q \psi_{fd}}{R^2 B_{equ}} u_q, \quad \tilde{T}_L = \frac{L_q^2}{R^2 J_{equ}} T_L$$

Among them, u_d and u_q respectively represent axis and quadrature axis stator voltage, i_d and i_q respectively represent axis and quadrature axis of the stator current, R is for stator winding resistance, L_d and L_q represent axis and quadrature axis stator inductance, $\psi_{fd} = 1.5\psi_f$ is for axial magnetic flux P_n , signify logarithmic, ω indicate motor angular frequency, J_{equ} on behalf of the equivalent moment of inertia of polar coordinates, T_L indicate external load torque, B_{equ} indicate the equivalent viscous damping coefficient.

Through the analysis of the type (1) we can know, when $\sigma = 10.5$, $\tilde{T} = 6$, the control parameter is set to $\tilde{u}_q = -x$, $\tilde{u}_d = 0$. The speed is closed-loop linear feedback control, and change from 1 to 500, the system Hopf bifurcate as shown in Figure 1.

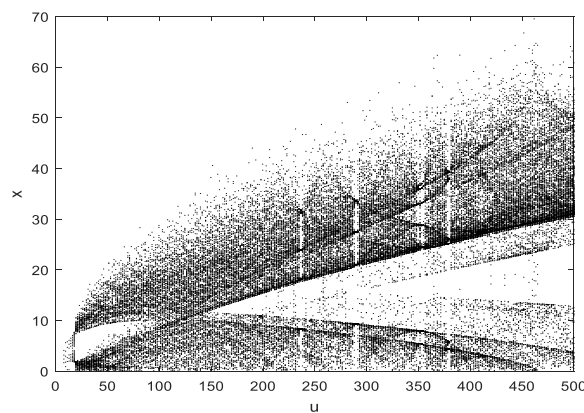
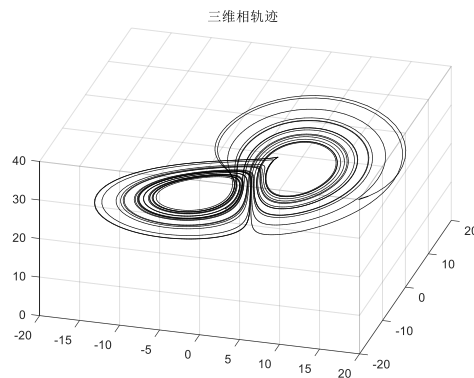
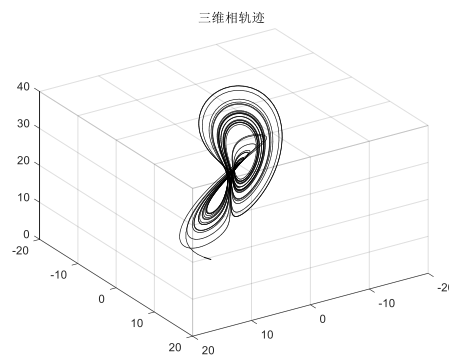


Figure 1. Bifurcation Diagram

When $\mu = 24.8$, using the method of order 4 *Runge–Kutta*, we can calculate the numerical solution of chaos model to get the phase trajectory of the system. As you can see phase trajectory within a bounded become disordered, which means it has entered into a state of chaos, as shown in Figure 2.



a) Azimuth 74°, Elevation angle 42°



b) Azimuth 57°, Elevation angle 38°

Figure 2. Three-dimensional Phase Trajectories for Different Viewing Angles

As the above picture shows, the system will fall into chaos motion state when its parameters and μ, σ and external disturbance \tilde{T}_L (external disturbance \tilde{T}_L will change as time goes on, so we can not accurately know the specific number) meet some conditions,, whose main performance is intense oscillation, unstable speed or torque control performance, and the irregular electromagnetic noise of the system, etc.

As we can see from the system dynamics equations (1), u_q, u_d can be used as a control input to eliminate chaos state and can make the system speed track realize the desired expectations. The next task is to design control law of the two variables.

3. Adaptive Robust Controller Design

According to the dynamic equation (1) there exist parameter uncertainty (structural uncertainty) and external disturbance (unstructured uncertainty) in the dynamic system, so it is necessary to take

different methods to handle them.

In order to better estimate the system parameters and control the chaos in the permanent magnet synchronous motor, the force u_1 is been inputted into speed differential equations according to the entrainment and migration control thought, the closed loop dynamics equation of permanent magnet synchronous motor system are given as follows:

$$\begin{cases} \dot{x} = \sigma(y-x) - \tilde{T}_L + u_1 \\ \dot{y} = (\mu - z)x - y + \tilde{u}_q \\ \dot{z} = -z + xy + \tilde{u}_d \end{cases} \quad (2)$$

Among them, $u_1, \tilde{u}_q, \tilde{u}_d$ as control input.

The system error of the variables:

$$\begin{cases} z_1 = x - x_d \\ z_2 = y - \alpha_1 \\ z_3 = z - z_d \end{cases} \quad (3)$$

Where z_1 represents speed tracking error, x_d represents the required speed by the system, z_2 represents the virtual control input difference, y represents virtual control input, α_1 represent virtual control input y control functions, z_3 represents d shaft current tracking error, z_d for the desired output d shaft current.

3.1 Design of Adaptive Parameter Estimator

An estimator needs to be designed to estimate unknown parameters. If $\hat{\sigma}$ is the estimate of the σ , $\tilde{\sigma}$ is the parameter estimation errors, which means $\tilde{\sigma} = \hat{\sigma} - \sigma$. If $\hat{\mu}$ is estimated value of μ , $\tilde{\mu}$ represent the parameter estimation error, which means $\tilde{\mu} = \hat{\mu} - \mu$. In order to make the parameter estimation with infinite delay, the design of adaptive parameter estimation discontinuous projection algorithm is as follows:

$$\dot{\hat{\sigma}} = \text{Proj}_{\hat{\sigma}}(z_1 z_2) \quad (4)$$

$$\dot{\hat{\mu}} = \text{Proj}_{\hat{\mu}}(x z_2) \quad (5)$$

Where:

$$\text{Proj}_{\hat{\theta}}(\bullet_i) = \begin{cases} 0 & \begin{cases} \hat{\theta} = \hat{\theta}_{\max} \text{ 且 } \bullet_i > 0 \\ \hat{\theta} = \hat{\theta}_{\min} \text{ 且 } \bullet_i < 0 \end{cases} \\ \bullet_i & \text{other} \end{cases} \quad (6)$$

And it has the following properties:

$$\hat{\sigma} \in L_{\infty}, \quad \tilde{\sigma}[\text{Proj}_{\hat{\sigma}}(z_1 z_2) - z_1 z_2] \leq 0 \quad (7)$$

$$\hat{\mu} \in L_{\infty}, \quad \tilde{\mu}[\text{Proj}_{\hat{\mu}}(x z_2) - x z_2] \leq 0 \quad (8)$$

3.2 The Design of Control Law u_1

Speed tracking control law u_1 is designed to make the pratical speed of the system to track the speed required. Nonlinear feedback control law is designed as follows:

$$u_1 = \dot{x}_d - \hat{\sigma}(y-x) - k_1 z_1 + \alpha_{1s} \quad (9)$$

Where $\dot{x}_d - \hat{\sigma}(y-x)$ is the feed-forward compensation term in the model, $-k_1 z_1$ is the linear robust feedback used to stabilize system nominal model. The α_{1s} is nonlinear robust feedback used to compensate the errors of parameter estimation and load torque disturbance. Then design $k_1 > 0$, error dynamic equation can be seen in the following:

$$\dot{z}_1 = \dot{x} - \dot{x}_d = -\tilde{\sigma}(y-x) - k_1 z_1 + \alpha_{1s} - \tilde{T}_L \quad (10)$$

3.3 Control the Design of Function α_1

Design the control function α_1 of the virtual control input y to ensure the output tracking performance. The virtual control law is designed as follows:

$$\alpha_1 = x \quad (11)$$

By substituting the second equation in equation (3) and equation (11) into equation (10), the following error equation can be obtained:

$$\dot{z}_1 = -k_1 z_1 + \alpha_{1s} - \tilde{\sigma} z_2 - \tilde{T}_L \quad (12)$$

Because α_{1s} can make as small as possible, so we need eliminate the influence of α_{1s} for $\tilde{\sigma} z_2 + \tilde{T}_L$ as much as possible. In addition, if the $\tilde{T}_L = 0$, when z_2 reduce to zero, z_1 will reduce to zero.

3.4 The Design of the Actual Control Law \tilde{u}_q

According to the third equation in equation (3), we can see that the time derivative of z_2 is $\dot{z}_2 = \dot{y} - \dot{\alpha}_1$. By bringing the second equation in equation (1) into the time derivative of z_2 , we can get:

$$\dot{z}_2 = \dot{y} - \dot{\alpha}_1 = (\mu - z)x - y + \tilde{u}_q - \dot{\alpha}_1 \quad (13)$$

Proposed control law is as follows:

$$\tilde{u}_q = -(\hat{\mu} - z)x + y + \dot{\alpha}_1 - k_2 z_2 \quad (14)$$

Put formula (14) into formula (13) we obtain $\dot{z}_2 = -\tilde{\mu}x - k_2 z_2$.

3.5 The Design of the Robust Feedback Item α_{1s}

Nonlinear robust feedback item α_{1s} is designed to eliminate the influence of $\tilde{\sigma} z_2 + \tilde{T}_L$ on the system stability. While $\tilde{\sigma} z_2 + \tilde{T}_L$ is unknown, but it has a definite boundary of determination h , which is

$|\tilde{\sigma} z_2 + \tilde{T}_L| \leq h$, we can choose a robust feedback as follows to overcome the instability causes actuator

jitter shortcomings according to the ideas of the sliding mode control:

$$\alpha_{1s} = -h \cdot \frac{h}{4\varepsilon} z_1 \quad (15)$$

Where ε is the bounded positive scalar of control precision, $\frac{h}{4\varepsilon} z_1$ is the continuous approximation function of $\text{sgn}(z_1)$, through which we can effectively solve the problem of jitter.

3.6 The Design of Control Law \tilde{u}_d

Nonlinear feedback control law is proposed as follows:

$$\tilde{u}_d = z - xy - k_3 z_3 + \dot{z}_d \quad (16)$$

Where $k_3 > 0$. Put formula (16) into the third equation of formula (3), then we can obtain:

$$\dot{z} = -k_3 z_3 + \dot{z}_d \quad (17)$$

Put formula (17) into the error dynamic equation $\dot{z}_3 = \dot{z} - \dot{z}_d$, then we can obtain $\dot{z}_3 = -k_3 z_3 + \dot{z}_d - \dot{z}_d$. The error dynamics equation of exponential stability are as follows:

$$z_3(t) = z_3(0) \exp(-k_3 t) \quad (18)$$

This ensures that the tracking error z_3 is global uniform stability, according to the above mentioned we know that the system state z will converge to the desired output trajectory z_d .

4. Stability Analysis

Using adaptive robust control law (14) and the parameter adaptive law (4) and (5), to ensure the prescribed transient and steady-state performance in the system output tracking of x , The tracking error is converged by a known function to no less than the index of convergence and convergence speed of $\sqrt{\frac{\varepsilon}{k_1}}$ and the convergence rate is not less than k_1 .

Select lyapunov functions:

$$V_s = \frac{1}{2} z_1^2 \quad (19)$$

Derivative of formula (19) available:

$$\begin{aligned} \dot{V}_s &= z_1 \dot{z}_1 \\ &= z_1 (-k_1 z_1 + \alpha_{1s} - \tilde{\sigma}_{z_2} - \tilde{T}_L) \\ &= -k_1 z_1^2 + z_1 (\alpha_{1s} - \tilde{\sigma}_{z_2} - \tilde{T}_L) \leq -k_1 z_1^2 + \varepsilon \end{aligned} \quad (20)$$

where

$$\begin{aligned} z_1 (\alpha_{1s} - \tilde{\sigma}_{z_2} - \tilde{T}_L) &= z_1 [-h \cdot \frac{h}{4\varepsilon} z_1 - \tilde{\sigma}_{z_2} - \tilde{T}_L] \\ &= -\frac{h}{4\varepsilon} z_1^2 - z_1 (\tilde{\sigma}_{z_2} + \tilde{T}_L) \\ &\leq -\frac{h}{4\varepsilon} z_1^2 + |z_1| \cdot |\tilde{\sigma}_{z_2} + \tilde{T}_L| \\ &\leq -\frac{h}{4\varepsilon} z_1^2 + |z_1| \cdot h - \varepsilon + \varepsilon \\ &= -(\frac{h}{2\sqrt{\varepsilon}} z_1 - \sqrt{\varepsilon})^2 + \varepsilon \leq \varepsilon \end{aligned} \quad (21)$$

Then

$$z_1^2 \leq |z_1(0)|^2 \exp(-2k_1 t) + \frac{\varepsilon}{k_1} [1 - \exp(-2k_1 t)] \quad (22)$$

From formula (22) we can see that as the tracking error is limited, the index converged to $\sqrt{\frac{\varepsilon}{k_1}}$ and the convergence rate is not less than k_1 so as to guarantee that the output tracking has specified transient and steady state performance.

Above results show that the proposed adaptive robust controller can guarantee the output tracking transient performance and tracking accuracy in the end. After a period the tracking error can be compressed into the scope of the provisions by reducing parameter can be any smaller.

Using adaptive robust control law (14) and the parameter adaptive law (4) and (5) to achieve asymptotic output tracking of x only in the presence of parameter uncertainties.

When $\tilde{T}_L = 0$, construct the Lyapunov function:

$$V_a = \frac{1}{2} z_1^2 + \frac{1}{2} \tilde{\sigma}^2 + \frac{1}{2} z_2^2 + \frac{1}{2} \tilde{\mu}^2 \quad (23)$$

Derivative of formula (23) available:

$$\begin{aligned} \dot{V}_a &= z_1 \dot{z}_1 + z_2 \dot{z}_2 + \tilde{\sigma} \dot{\tilde{\sigma}} + \tilde{\mu} \dot{\tilde{\mu}} \\ &= z_1 (-\tilde{\sigma} z_2 - k_1 z_1 + \alpha_{1s}) + z_2 (-\tilde{\mu} x - k_2 z_2) + \tilde{\sigma} \text{Proj}_{\tilde{\sigma}}(z_1 z_2) + \tilde{\mu} \text{Proj}_{\tilde{\mu}}(x z_2) \\ &= -k_1 z_1^2 - k_2 z_2^2 + z_1 \alpha_{1s} + \tilde{\sigma} (\text{Proj}_{\tilde{\sigma}}(z_1 z_2) - z_1 z_2) + \tilde{\mu} (\text{Proj}_{\tilde{\mu}}(x z_2) - x z_2) \\ &\leq -k_1 z_1^2 - k_2 z_2^2 \end{aligned} \quad (24)$$

If the unknown parameter is a constant, $\dot{\tilde{\sigma}} = \dot{\tilde{\sigma}}, \dot{\tilde{\mu}} = \dot{\tilde{\mu}}$ can be obtained. So for all time, there is

$V_a(t) \leq V_a(0)$, and we can obtain that $z_1 \in L_\infty, z_2 \in L_\infty, \tilde{\mu} \in L_\infty$.

$$\int_0^t k_1 z_1^2(v) + k_2 z_2^2(v) dv \leq -\int_0^t \dot{V}_a(v) dv = -[V_a(t) - V_a(0)] \leq V_a(0) \quad (25)$$

which means that $z_1 \in L_2, z_2 \in L_2$. From formula (15) and formula (17) we can get $\dot{z}_1 \in L_\infty, \dot{z}_2 \in L_\infty$ and z_1, z_2 is uniform continuous. Through Barbalat lemma, asymptotic output tracking only achieved in the presence of parameter uncertainties.

Above results show that the proposed adaptive robust controller can realize asymptotic output tracking only in the presence of parameter uncertainties.

5. Simulation Calculation Results

Parameters used in the simulation test of the permanent magnet synchronous motor are as follows: The value of the stator resistance is $R = 2.6\Omega$. Inductance values are $L_d = L_q = 0.05H$, $L_a = 0.05H$. The magnetic poles logarithmic is $p_n = 4$. The rotor flux amplitude is $\psi_f = 0.48wb$. The equivalent inertia is $J_{equ} = 2.627 \times 10^{-5} kg \cdot m^2$. Equivalent viscous friction coefficient is $B_{equ} = 1.43 \times 10^{-2} Ns$.

$\sigma = 10.5$, $\mu = 24.8$ can be obtained by simple calculation, at the same time the system is in a state of chaos movement.

5.1 Track Constant Desired Output

Set the x control target as $x_d = 6$ and the z as $z_d = 0$. The simulation results is mainly used to track the constant desired output trajectory. If the external load torque disturbance is

$\tilde{T}_L = 6.0 + 0.1\sin(t)$, the boundary of the $\hat{\sigma}$ is $[0, 10]$, the boundary of the $\hat{\mu}$ is $[0, 50]$, $k_1, k_2, k_3 = 5.0$ represents the feedback gain, ε represents tracking accuracy. When it is reduced, tracking error will be smaller accordingly. When ε is further reduced, however, the controller robust part of the feedback gain get bigger, leading to serious control input jitter, and system instability. Therefore, ε is always present with the lower limit, so that we can restruct the tracking accuracy. ε needed to be an appropriate value, and the value of ε is 0.1 here. In order to clearly illustrate the control effect, when the time is 50 seconds, the controller works, and its state variables is shown in Figure 3.

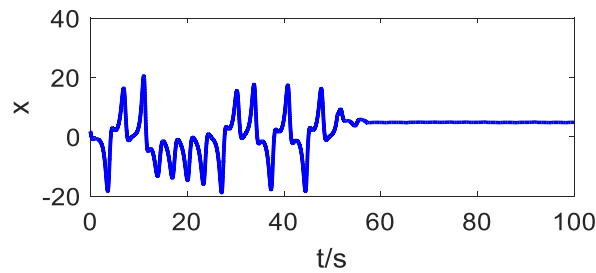


Figure 3. The Controller's System Status Curve that Takes Effect at 50 Seconds

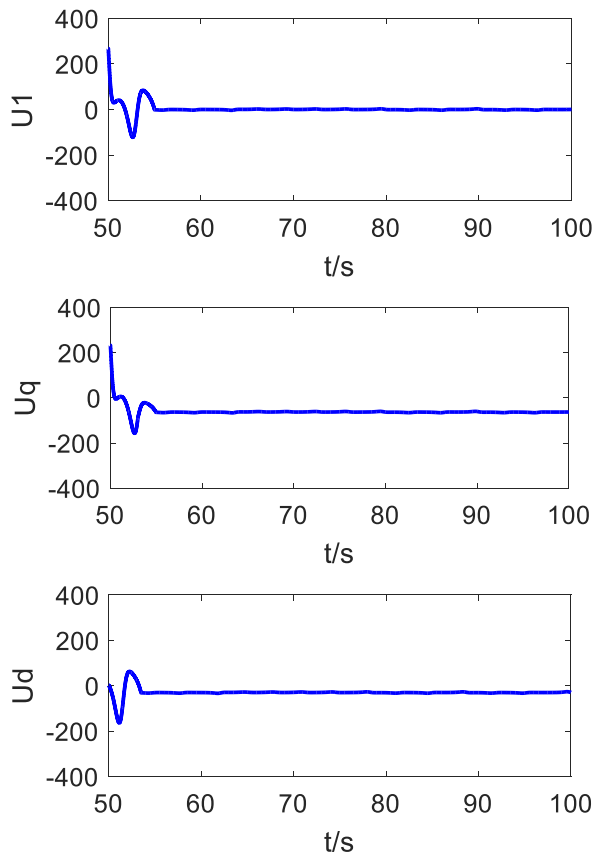


Figure 4. After 50 Seconds to Control the Input Curve

Based on the above analysis we can know, the system was driven to be a stable equilibrium state, as is shown in Figure 3. System control input as shown in Figure 4. System parameter estimation as shown in Figure 5. And from this figure we can see that, the parameter estimate just converged to a steady value. When \tilde{T}_L get bigger, using adaptive control law (Hu, Liu, Ma, & Ullah, 2015) the parameter estimation will diverge, so the controller is not stable. Controller proposed in this paper, however, is only adopted the discontinuous projection method to improve the adaptive law, parameter estimation can be kept within a certain range, rather than diverge. Therefore, it ensures the finite model of uncertainty and the stability of the whole system. Figure 6 is the adaptive robust controller and the comparison curve of commonly nonlinear feedback controller with off-line parameter estimation. Assume the parameter estimation $\sigma = 9.5, \mu = 23.5, \tilde{T}_L = 5.0$, we can see from the figure 6 that the speed tracking error is always in the steady state error range ($\sqrt{\frac{\varepsilon}{k_1}} \approx 0.14$, by calculating), and when the parameter estimation deviates from the value of the real, general nonlinear feedback controller has more tracking error. As a result, the adaptive robust nonlinear feedback controller to external load torque disturbance has better robustness, and have better effect in driving the speed to expectations.

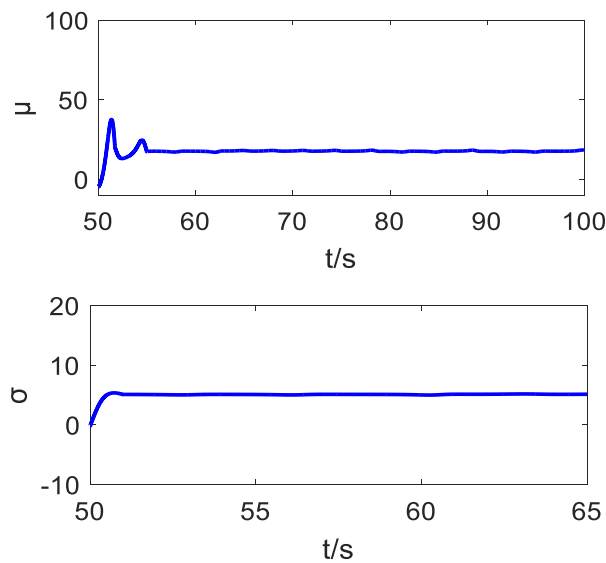


Figure 5. System Parameter Estimation Curve after 50 Seconds

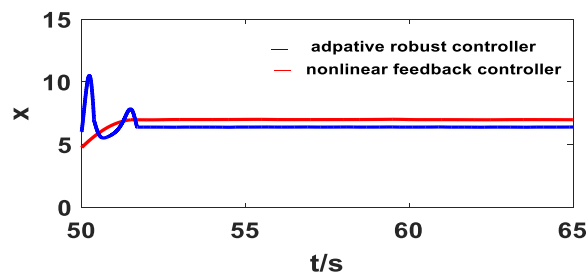


Figure 6. Comparison Curve of Two Controllers

5.2 Track Sine Curve Desired Output

Set the control target as $x_d = 15\sin(1.57t)$ of x , z control objectives are set for $z_d = 0$. Other system parameters choices are equal to the desired output of the tracking constant in the last section. Controller also has effect at the time of 50 seconds, state variables are shown in Figure 7. From this figure we can see that the system state converged to the desired trajectory after the transition period of the oscillation.

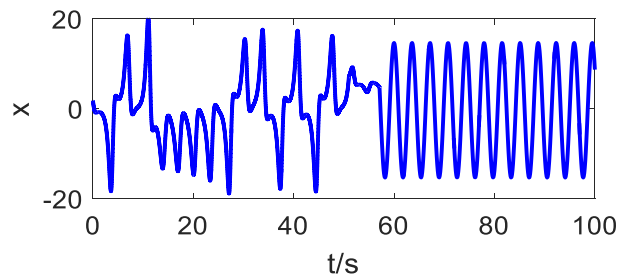


Figure 7. The Controller's System Status Curve that Takes Effect at 50 Seconds

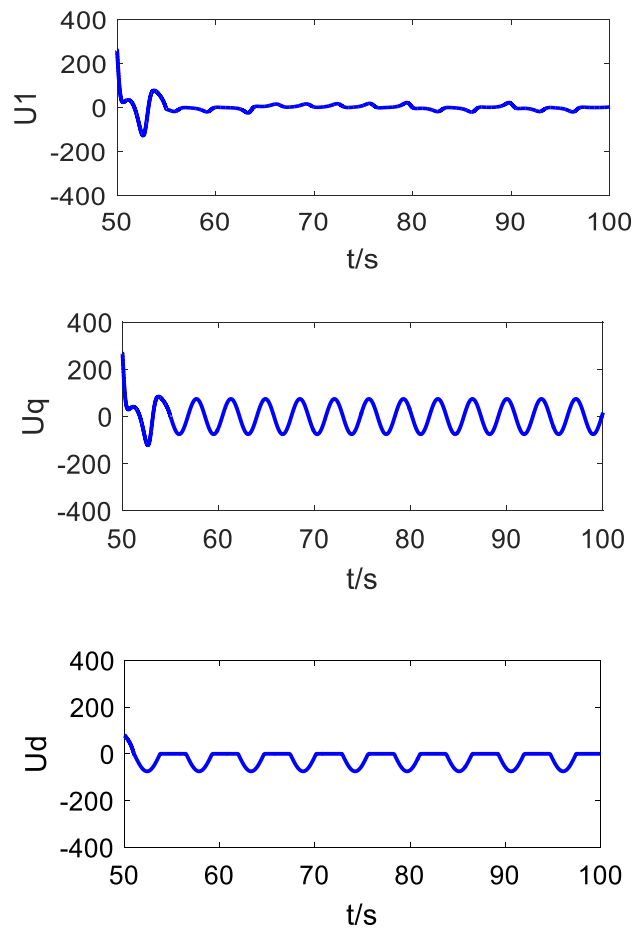


Figure 8. After 50 Seconds to Control the Input Curve

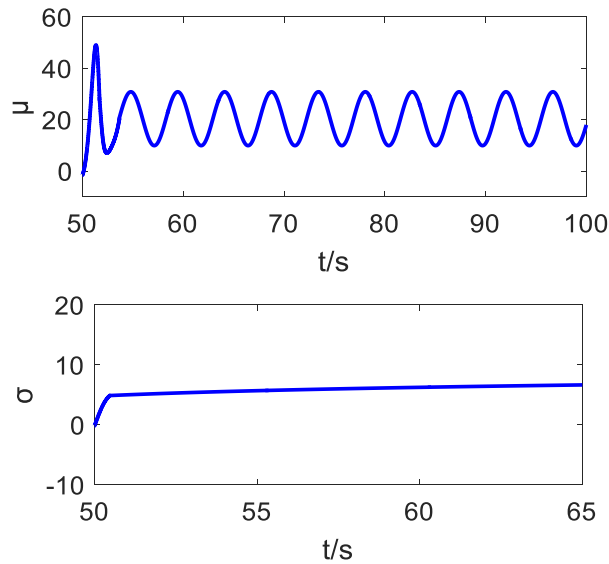


Figure 9. 50 Seconds after the System Parameter Estimation Curve

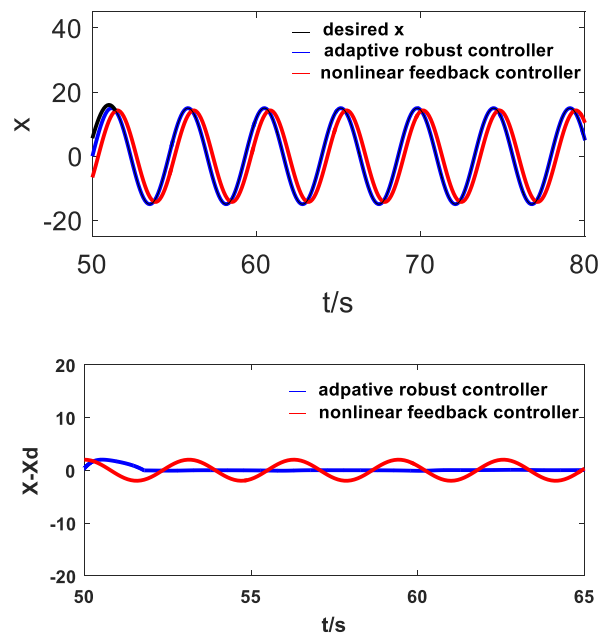


Figure 10. Comparison Curve of Two Controllers

Figure 8 shows the control input. System parameter estimation is in Figure 9 from which we can see there exist the estimated μ oscillation and σ estimated asymptotically converge to its real value, but there is estimation error also. Both estimates, however, remain within a certain range, without divide, which means the uncertainty of the bounded model, thus we can compensate that by stability of the controller. Figure 10 is the comparison curves of the two controllers from which we can see the velocity error of general nonlinear feedback controller is far bigger than that of the adaptive robust controller, which further verify the strong robustness of the adaptive robust controller.

6. Conclusion

This paper presents a chaotic control method based on adaptive robust controller, which is used to eliminate or suppress parameter uncertain chaos in permanent magnet synchronous motor system, and at the same time, considering the external load torque disturbance, the speed accurately is driven to the prescribed trajectory. Adaptive robust controller is designed which proved by Lyapunov method that the proposed controller can realize the transient and steady state performance. From two aspects that track constant desired output and track sine curve desired output to verify the effectiveness and superiority of the method, and the simulation results show that this method can eliminate the chaos and achieve good tracking accuracy.

References

- Babaei, M., Nazarzadeh, J., & Faiz, J. (2008). Nonlinear feedback control of chaos in synchronous reluctance motor drive systems. In *Proceedings of IEEE International Conference on Industrial Technology*, 2008, pp. 1-5. <https://doi.org/10.1109/ICIT.2008.4608524>
- Chua, K. T., & Chen, J. H. (2003). Modeling, analysis and experimentation of chaos in switched reluctance drive system. *IEEE Trans. Circuits Syst. I: Fundam. Theory Appl.* 50(3), 712-716. <https://doi.org/10.1109/TCSI.2003.811030>
- Hemail, N. (1994). Strange attractors in brushless DC motor. *IEEE Trans. Circuits Syst. I: Fundam. Theory Appl.* 41(1), 40-45. <https://doi.org/10.1109/81.260218>
- Hu, J., Liu, L., Ma, D., & Ullah, N. (2015). Adaptive nonlinear feedback control of chaos in permanent magnet synchronous motor system with parametric uncertainty. *Proc. Inst. Mech. Eng. Part C: J. Mech. Eng. Sci.* 229(12), 2314-2323. <https://doi.org/10.1177/0954406214557344>
- Jing, Z., Yu, C., & Chen, G. (2004). Complex dynamics in a permanent-magnet synchronous motor model. *Chaos Solitons Fractals*, 22, 831-848. <https://doi.org/10.1016/j.chaos.2004.02.054>
- Krishnendu Chakrabarty, & Urmila Kar. (2013). Bifurcation phenomena in Induction motor. In *Proceedings of Annual IEEE India Conference*. <https://doi.org/10.1109/INDCON.2013.6725891>
- Li, Z., Park, J. B., Joo, Y. H., Zhang, B., & Chen, G. (2002). Bifurcations and chaos in a permanent magnet synchronous motor. *IEEE Trans. Circuits Syst. I: Fundam. Theory Appl.* 49(3), 383-387. <https://doi.org/10.1109/81.989176>
- Mark, A. P., Vairamani, R., & Irudayaraj, G. C. R. (2014). Mathematical modeling and analysis of different vector controlled CSI Fed 3-phase induction motor. *J. Appl. Math.* 2014, 623982-1-623982-13. <https://doi.org/10.1155/2014/623982>
- Ott, E., Grebogi, C., Yorke, J. A. (1990). Controlling Chaos. *Phys. Rev. Lett.* 64(11), 1196-1199. <https://doi.org/10.1103/PhysRevLett.64.1196>
- Ren, H. P., & Ding, L. (2006). Nonlinear feedback control of chaos in permanent magnet synchronous motor. *IEEE Trans. Circuits Syst. II: Express Briefs*, 53(1), 45-50. <https://doi.org/10.1109/TCSII.2005.854592>

- Saberi Nik, H., & Gorder, R. A. (2013). Competitive modes for the Baier-Sahle hyperchaotic flow in arbitrary dimensions. *Nonlinear Dyn.* 74, 581-590. <https://doi.org/10.1007/s11071-013-0990-9>
- Saberi Nik, H., Gorder, R. A., & Gambi, G. (2015). The chaotic Dadras-Momeni system: control and hyperchaotification. *IMA J. Math. Control Inf.* (2015). <https://doi.org/10.1093/imamci/dnu050>
- Sun, W., Gao, H., & Kaynak, O. (2013). Adaptive backstepping control for active suspension systems with hard constraints. *IEEE/ASME Trans. Mechatron.* 18(3), 1072-1079. <https://doi.org/10.1109/TMECH.2012.2204765>
- Underwood, S. J., & Husain, I. (2010). Online parameter estimation and adaptive control of permanent magnet synchronous machines. *IEEE Trans. Ind. Electron.* 57(7), 2435-2443. <https://doi.org/10.1109/TIE.2009.2036029>
- Wang, Z., & Chau, K. T. (2009). Design, analysis, and experimentation of chaotic permanent magnet DC motor drives for electric compaction. *IEEE Trans. Circuits Syst. II: Express Briefs*, 56(3), 245-249. <https://doi.org/10.1109/TCSII.2009.2015371>
- Xu, L., & Yao, B. (2001). Adaptive robust precision motion control of linear motors with negligible electrical dynamics: theory and experiments. *IEEE/ASME Trans. Mechatron.* 6(4), 444-452. <https://doi.org/10.1109/3516.974858>
- Yao, B., Bu, F., Reedy, J., & Chiu, G. T. C. (2000). Adaptive robust motion control of single-rod hydraulic actuators: theory and experiments. *IEEE/ASME Trans. Mechatron.* 5(1), 79-91. <https://doi.org/10.1109/3516.828592>
- Yao, B., Hu, C., & Wang, Q. (2012). An orthogonal global task coordinate frame for contouring control of biaxial systems. *IEEE/ASME Trans. Mechatron.* 17(4), 622-634. <https://doi.org/10.1109/TMECH.2011.2111377>
- Yao, J., Jiao, Z., & Ma, D. (2014). Extended-state-observer-based output feedback nonlinear robust control of hydraulic systems with backstepping. *IEEE Transactions on Industrial Electronics*, 61(11), 6285-6293. <https://doi.org/10.1109/TIE.2014.2304912>
- Yao, J., Jiao, Z., & Ma, D. (2015). A practical nonlinear adaptive control of hydraulic servomechanisms with periodic-like disturbances. *IEEE/ASME Transactions on Mechatronics*, 20(6), 2752-2760. <https://doi.org/10.1109/TMECH.2015.2409893>
- Yao, J., Jiao, Z., Ma, D., & Yan, L. (2014). High-accuracy tracking control of hydraulic rotary actuators with modeling uncertainties. *IEEE/ASME Trans. Mechatron.* 19(2), 633-641. <https://doi.org/10.1109/TMECH.2013.2252360>
- Zhang, Z., Chau, K. T., & Wang, Z. (2013). Analysis and stabilization of chaos in the electric-vehicle steering system. *IEEE Trans. Veh. Technol.* 62(1), 118-126. <https://doi.org/10.1109/TVT.2012.2217767>